CONFERENCE PRE-PRINT

FAST: A FUSION ENERGY SYSTEMS INTEGRATION TEST FACILITY

[1]A. EJIRI, [2]N. ASHIKAWA, [3]T. FUJITA, [4]K. HANADA, [5]K. IBANO, [6]H. IGAMI, [2]Y. KUME, [2]S. KONISHI, [1]Y. ONO, [2]K. SEKO, [7]Y. TAKASE, [8]H. TANAKA, [9]K. TOBITA, [2]T. TSUJIMURA, [10]H. TSUTSUI

[1]The University of Tokyo, Kashiwa, 277-8561, Japan
[2]Kyoto Fusioneering Ltd., Tokyo, 100-0004, Japan
[3]Nagoya University, Nagoya, 464-8603, Japan
[4]Kyushu University, Kasuga, 816-8580, Japan
[5]The University of Osaka, Suita, 565-0871, Japan
[6]National Institute for Fusion Science, Toki, 509-5292, Japan
[7]Tokamak Energy Ltd, Oxfordshire OX14 4SD, UK
[8]Kyoto University, Kyoto, 615-8540, Japan
[9] Tohoku University, Sendai, 980-8579, Japan
[10]Institute of Science Tokyo, Tokyo 152-8550, Japan
Email: ejiri@k.u-tokyo.ac.jp

Abstract

FAST (Fusion by Advanced Superconducting Tokamak) is a project being proposed as a facility for R&D, testing, and to demonstrate integration of systems necessary for a Deuterium Tritium (DT) fusion energy reactor. The required specifications for FAST are: DT fusion power of $50-100$ MW, neutron wall loading of $0.3-1$ MW/m^2, discharge duration of about 1000 s, full-power operation time of about 1000 hrs (same order as ITER). These are identified as required and also sufficient for the near-term R&D of the tritium breeding and power extraction blanket to verify the integrity of the fusion system. Since we would like to demonstrate electricity generation technology using the thermal energy extracted from blankets in the 2030's, minimization of the cost is essential, because it determines the necessary funding and the construction period. Integrated fusion fuel cycle and safety features as an energy plant that will fill the technical gap toward net positive energy generation plant is another mission, while the system integration has the highest priority. A quasi-zero-dimensional parameter survey has been carried out to find the parameter region necessary to satisfy the above specifications with the minimum device cost. It was found that a low aspect ratio (A ~ 2.2), compact (major radius ~ 2.0 m) tokamak with high temperature superconductor (HTS) magnets and neutral beam injection (NBI) power of about 50 MW (with the energy of 500 keV) offers a possible design window.

1. INTRODUCTION

One of most important issues for the development of a Deuterium Tritium (DT) fusion energy reactor is the integration of systems. It is necessary to demonstrate power generation using fusion energy and tritium breeding by blankets installed near the plasma. Therefore, sufficient fusion power and neutron wall loading are necessary. In order to demonstrate the technical feasibility, DT burning periods should be long enough so that the heat exchange loop is in thermal equilibrium. Considering these requirements, the target parameters in the FAST project are DT fusion power of 50-100 MW, neutron wall loading of 0.3-1 MW/m^2 and discharge duration of about 1000 s [1]. The project aims to demonstrate the power generation by the 2030s. Compared to these requirements, the priorities of high energy gain and tritium breeding ration above one and a long operational period, which are necessary for a demo reactor, are not so high. A full-power operation time of about 1000 hrs (same order as ITER) is the target. Since the 2030's is a near future, minimization of the cost is essential, because it determines the necessary funding and the construction period. A quasi-zero-dimensional parameter survey has been carried out to find the parameter region necessary to satisfy the above specifications with the minimum device cost. Since NBI (Neutral Beam Injection) is the main heating and current drive tool, beam-thermal reaction can be significant. The three types of reactions: thermal-thermal, beam-thermal, beam-beam are investigated for various injection and target conditions to find the responses on fusion power and driven current.

2. PLASAMA MODEL AND COST MODEL

A quasi-zero-dimensional plasma model has been developed [2]. Power balance is calculated using the hybrid confinement time, in which the energy confinement times of spherical tokamaks and high aspect ratio tokamaks are interpolated in the inverse aspect ratio $\epsilon = 1/A$ [3]. The interpolation is necessary to scan the aspect ratio in the region around $1.6 - 2.7$. The energy confinement time is written as

$$\tau_{Hybrid} = f_{0.9}\left(\gamma\tau_{Petty} + (1-\gamma)\tau_{NSTX}\right), \quad \text{where } \gamma \equiv \frac{\epsilon_1 - \epsilon}{\epsilon_1 - \epsilon_2},\ \epsilon_1 = \frac{1}{1.6}, \epsilon_2 = \frac{1}{2.667}\ . \qquad \text{Eq. (1)}$$

Here $f_{0.9} = 0.9$ is the energy confinement time enhancement factor. See Ref. [3] for τ_{Petty} and τ_{NSTX}. The power balance is written as

$$\frac{W_{store}}{\tau_{Hybrid}} = f_{0.9}(P_{NBI} + P_{\alpha th} + P_{\alpha NB}) - P_{rad}\ . \qquad \text{Eq. (2)}$$

Here, W_{store}, P_{NBI}, $P_{\alpha th}$, $P_{\alpha NB}$ and P_{rad} represent stored energy, D-NBI power, α-particle heating due to the reactions among thermal components, that due to the reactions between slowing down beam components and thermal components and the radiation power, respectively. Once the size and temperature and density profiles are given, the deposition profile and the shine through of NBI, of which energy is fixed to be 500 keV in this section, can be calculated and slowing down energy distribution function can also be calculated. The α-particle and neutron generation and radiation profiles are calculated and integrated to yield each term in Eq. (2). The density ratios of D, T, He and Ar are fixed as $n_D = n_T = \frac{0.834}{2} \times n_e, n_{He} = 0.057 \times n_e,\ n_{Ar} = 0.029 \times n_e$, which results in the effective charge of $Z_{eff} = 2.0$.

Figure 1 (a) shows the temperature and density profiles, of which shapes are fixed as

$$T_e(\rho) = T_i(\rho) = T_0 \times (0.95(1-\rho^{1.6})^2 + 0.05(1-\rho^{10}))\ , \qquad \text{Eq. (3)}$$

$$n_e(\rho) = \frac{n_{DT}}{f_{DT}} = \overline{n_e}(0.525(1-\rho^{2.6})^2 + 0.879(1-\rho^6))\quad , \qquad \text{Eq. (4)}$$

$$j(\rho) = j_0(0.7(1-\rho^2)^2 + 0.3(1-\rho^2)^{0.5})\ . \qquad \text{Eq. (5)}$$

Here, T_0, $\overline{n_e}$ and j_0 are free parameters, which are determined as follows. $f_{DT} = 0.84$ represents the ratio of DTs to electrons. The density $\overline{n_e}$ is given by a normalized density, which is normalized by the Greenwald density. The temperature T_0 is adjusted to yield W_{store}. Since these quantities depend on each other, we need iteration to find the parameters. Similarly, the plasma current is obtained. The plasma current I_p consists of NBI driven current I_{NB} and bootstrap current I_{BS} and I_p is written as

$$I_p = f_{0.9}I_{NB} + I_{BS}. \qquad \text{Eq. (6)}$$

Here, $f_{0.9}$=0.9 represents unknow degradation of efficiency. Note that shine through loss and prompt orbit loss are already included in I_{NB}. Figure 1(b) and (c) show the current and heating power profiles, respectively. The NBI driven local current density is calculated using the NB deposition (i.e., ionization) profile and a formula for the current drive efficiency [4]. The bootstrap current density is calculated from a formula in [5] using the poloidal magnetic field profile using the current density (Eq. (5)). The total currents (I_p, I_{NB} and I_{BS}) are calculated by the area integration on the elliptical poloidal cross section. DT reaction rate is calculated using a formula in [6]. For simplicity, the current density profile shape is fixed (Eq. (5)), although the driven current density profiles are calculated (see solid and dotted curve in Fig. 1(b)). Using the neutron generation profile, the outboard neutron wall loading is calculated through Monte Carlo calculations, which shows a maximum n_{WLmax} at the midplane (Fig. 1(d)). Inboard blankets will not be installed in FAST.

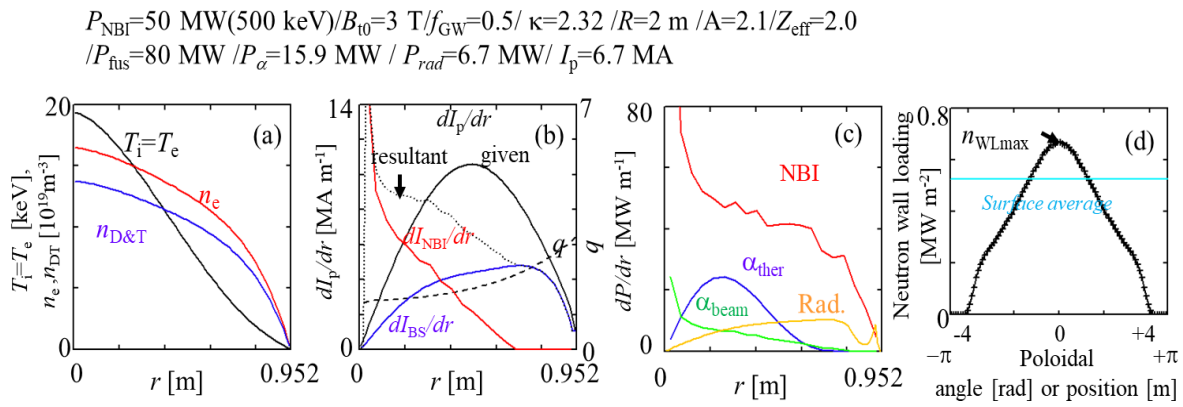

FIG. 1. Temperature and density profiles (a), current profiles (b), and power deposition profiles (c). The horizontal axis represents the minor radius at midplane. (d) shows the neutron wall loading as a function of the poloidal angle on a sphere.

The device cost is estimated by summing up the component costs using given unit volume costs as in the past works [7, 8]. While the plasma shape is determined from the major radius R, minor radius $a = R/A$ and elongation κ, most of the outer component thicknesses are fixed as indicated in Fig. 2. One of the features of the design is that the inboard blankets are removed, and the inboard shield thickness is thinner than many other reactor designs. The thinner inboard shield is feasible when we consider the short full-power operation time of about 1000 hrs.

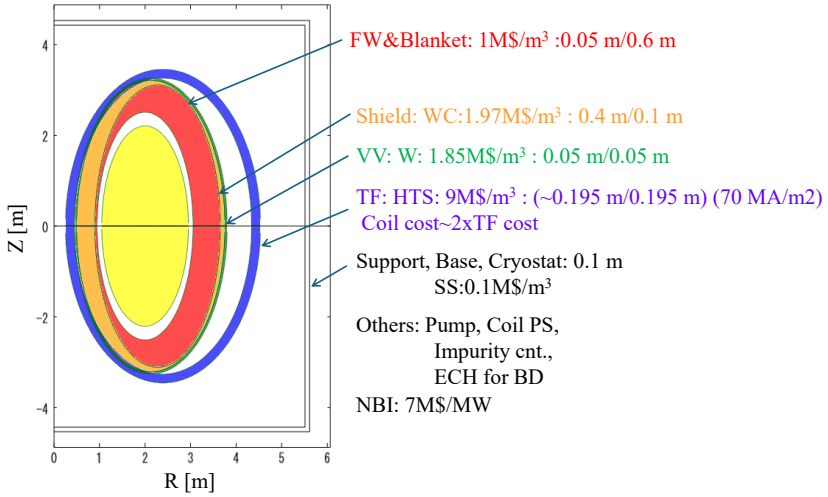

FIG. 2. Poloidal cross-section of the device showing the radial build. The unit volume cost for representative components and their inboard and outboard midplane thicknesses are also shown.

The maximum toroidal magnetic field is fixed to be 13.4 T (at the major radius of $R - a - 0.6$ m, where 0.6 m represents the distance between the coil and the plasma at the inboard side), and the current density across the coil is 70 MA/m^2. These specifications seem to be reasonable when we adopt state of art high temperature superconductor technology. Then the coil volume and cost are calculated from the position and these constraints. It should be noted that the magnetic field strength at the plasma centre increases with R and A. This A dependence is the opposite of the volumes of shield, blanket and etc. As a result, the sum of toroidal field cost and the other components' cost tends to be insensitive to A. The total device cost becomes a strong function of R and P_{NBI}.

3. PERFORMANCES AND DEVICE COST

By using the models described in the previous section, fusion power P_{fus} and maximum neutron wall loading n_{WLmax} are calculated for a given parameter set: R, $A = \frac{R}{a}$, κ, f_{GW} and P_{NBI}. Here, f_{GW} represents the density normalized by the Greenwald density. Thus, the plasma and device cost are functions of these five free parameters. We performed five-dimensional parameter space survey by random sampling in this space. Figure 3 shows resultant n_{WLmax}, P_{fus} as functions of R, A, f_{GW}. Here κ dependences are not shown, because the highest κ (premitted from the viewpoint of stability) is always more preferable than lower κ cases. n_{WLmax} and P_{fus} become maximum around $A = 2.1 - 2.2$. This is due to the feature of the energy confinement time and the constraint of the maximum toroidal field strength [2]. Both n_{WLmax} and P_{fus} increases with R, but n_{WLmax} starts to saturate at large R. This can be interpreted by the volume effect. f_{GW} dependence shows a gentle maximum. A high f_{GW} results in a high I_{BS}, while a low f_{GW} results in a high I_{NB}. It seems that f_{GW} is not a parameter to optimize, but it is a parameter to characterize the plasma and device. A very low f_{GW} leads to a beam-driven neutron irradiation reactor, where NBI is the main tool to sustain the plasma, while a very high f_{GW} leads to a self-sustained demo reactor. The FAST reactor is located between these two extrema.

If we set the target as $n_{WLmax} = 0.7\ \mathrm{MW/m^2}$ and $P_{fus} = 70$ MW, then we obtain the parameter sets with near minimum cost. The obtained parameters are $R \sim 2.0$ m, $A \sim 2.2$, $\kappa \sim 2.3$, $f_{GW} \sim 0.5$. $P_{NBI} \sim 50$ MW, and the device cost is about 800 M$, excluding BOP (Balance Of Plant) and the first of a kind cost enhancement. These optimum parameters will vary when we change the target n_{WLmax} and P_{fus}. Figure 4 shows the map in n_{WLmax}–P_{fus} plane. The colour indicates the minimum cost at each point (i.e. in each pixel) (a) or A which yields the minimum cost (b). A valley-like structure (dashed curve) can be seen in Fig. 4(a), which is a guideline for the appropriate combinations of n_{WLmax} and P_{fus}. When we want to increase P_{fus} without changing n_{WLmax}, a higher cost is necessary, and a lower aspect ratio A should be chosen according to Figs. 4(a) and (b). Thus, the combination of n_{WLmax} and P_{fus} on the valley is a guideline for the selection of n_{WLmax} and P_{fus}. One of the uncertainties on the selection arises from the relative cost of NBI. We investigated the case where the NBI cost per unit power increases by $\pm$ 30 %. Obviously, a lower (or a higher) NBI power is selected to minimize the cost when the NBI cost increases (or decreases). It should be noted that the optimum A is mainly determined by the feature of the hybrid energy confinement time, and we tried different interpolation methods, and the optimum A can varies by about 0.1 depending on the interpolation methods.

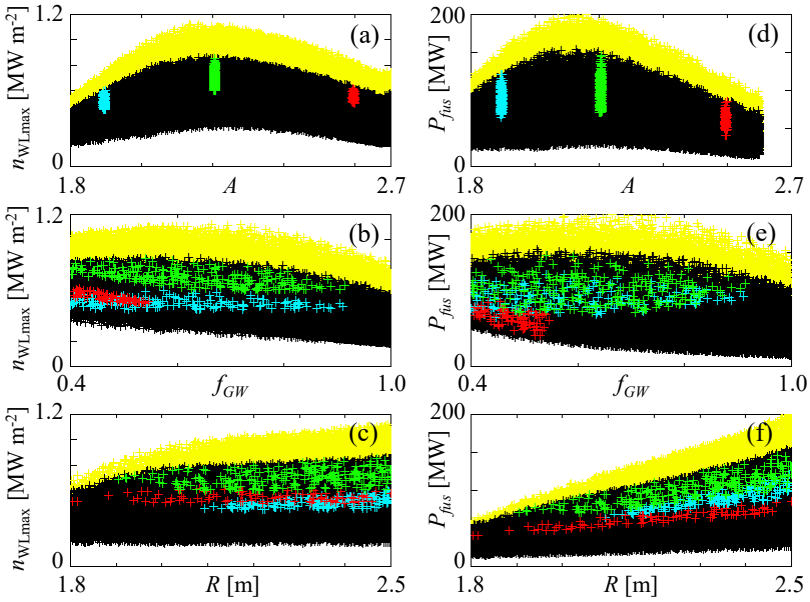

FIG. 3. Maximum neutron wall loading n_{WLmax} as functions of A, f_{GW} and R (a)–(c), and fusion power P_{fus} (d)–(f). The cyan (A≈1.9), green (A≈2.2) and red (A≈2.6) represents the cases of certain As with relatively high n_{WLmax} (> 0.45, 0.6, > 0.55, respectively). The external heating power is $P_{NBI} = 50$ MW, while the yellow points in the background show the cases with $P_{NBI} = 57$ MW.

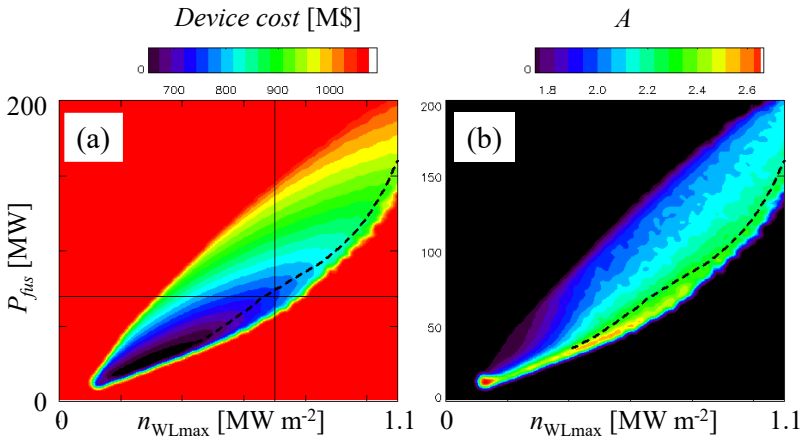

FIG. 4. Contour plots of device cost (a) and A (b) in the n_{WLmax}–P_{fus} plane. The dashed curves indicate the traces of cost valley. In (a) the lines of $n_{WLmax} = 0.7\ MW/m^2$ and $P_{fus} = 70$ MW are shown. The red (a) or black (b) background represents the region where no parameter sets satisfying the n_{WLmax} and P_{fus} are found.

In the above investigation, we did not consider the time evolution, but in practice, accessibility (i.e., discharge scenario) to the operation point should be considered. Particularly, it is important to start-up the plasma current, which is sustained by NB and bootstrap current. The latter two are those we considered (see. Eq. (3)). Since we consider a discharge duration of about 1000 s, it is also important to access a burning plasma within an appropriate time period. In order to startup the plasma current a central solenoid (CS) with a flux swing of 15 Vs and an EC power of 10 MW are introduced. We performed a time-dependent transport analysis, to find a discharge scenario. The EC power is used for the initial plasma start-up and initial plasma current ramp-up, and CS is used to ramp the plasma current after the EC power injection. Then the plasma density is increased, and NB injection starts. These induce not only NB-driven current but also the bootstrap current. Fusion burn starts and further bootstrap current is induced. With this scenario a plasma current of about 6 MA can be achieved. The CS flux and EC power are used mainly at the initial start-up phase, which takes less than about 60 s.

4. EFFECT OF NBI AND TARGET PLASMA CONDITIONS

In a low density plasma, fast ions generated by NBI show a long slowing down time, and the fast ion density and beam-thermal reaction rate increase. In the previous section we consider equal D-T ratio in target plasmas, and D-NBI, but we may choose other conditions. In order to maximize P_{fus}, the other conditions may be preferable. In this section, we scan the following parameters: ratio of D- and T- NBI powers: $P_D/(P_D + P_T)$, D/T ratio in the target plasma: $n_D/(n_D + n_T)$, injection angles: θ_D and θ_T with respect to the magnetic field. The NBI energies are also scanned later. The total NBI power is fixed to be 50 MW, and electron density and temperature are fixed to be $n_e = 1.2 \times 10^{20}\ 1/\mathrm{m}^3$, $T_e = T_D = T_T = 12.5$ keV (for the reference case), and the plasma volume is 40 m^3. Spatial profiles are not considered, that is, we consider zero-dimensional situations. In contrast, three-dimensional velocity distribution functions for the target thermal plasma, and the slowing down D- and T- fast ions (i.e., beam components) are calculated, and DT-reactions between them are calculated. In addition, beam driven current parallel to the magnetic field is calculated. Figure 5 shows distribution functions for a case. Energy distribution functions and two-dimensional velocity distribution function for D- and T- beam components are shown. The injection angles are shown by dashed lines. The fast ions show slowing down and pitch angle scattering. In addition, Larmor motion effect, which makes the perpendicular velocities axisymmetric with respect to the magnetic field, is considered.

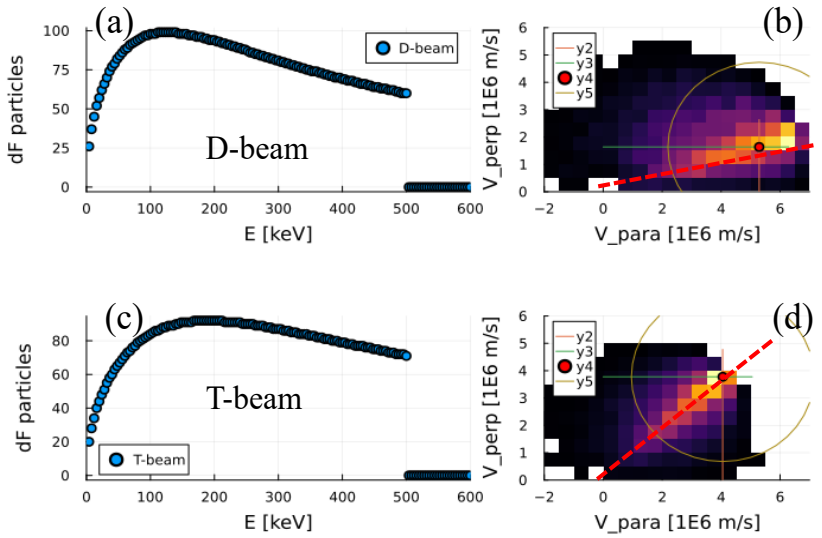

FIG. 5. Energy distribution function (i.e. number of particles in energy bins) (a), and 2-D velocity distribution (b) for D-beam component. Figure (c) and (d) show those for T-beam component. The NBI energies are 500 keV, and the injection angles are shown by red dashed lines in (b) and (d). The circles in (b) and (d) show the constant velocity ($\sim 3 \times 10^6 m/s$) from some points. This relative velocity corresponds to that of maximum DT reaction.

The parameters: $P_D/(P_D + P_T)$, $n_D/(n_D + n_T)$ and θ_D and θ_T are scanned by random samplings. Figure 6 shows the dependences of fusion powers P_{fus}s and NB driven currents I_{NB}s. Figures (a)-(d) show the reference cases, while Figs. (e) and (f) show much low density cases. The dependences of the reference cases are reasonable. The thermal-thermal reaction shows a maximum at $n_D/(n_D + n_T) = 0.5$, while beam thermal shows maxima at $n_D/(n_D + n_T) = 0$ (or 1) for D-beam (or T-beam). For a give NBI power, D-NBI shows a higher fusion power and a higher driven current, when the NBI-power and energy E_{beam} are given. This is due to the fact that the faster velocity for the D-NBI leads to a longer slowing down time and a higher beam component density. These results in a higher fusion power and a higher NB driven current as shown in Figs. 6(a) and 6(b). Due to this effect the optimum ratio of $n_D/(n_D + n_T)$ becomes less than 0.5 (Fig. 6(c)). The NBI injection angle of $\theta_D = \theta_T = 0$ is the optimum in terms of a higher drive plasma current (Fig. 6(d)).

These are the cases considered in FAST, where beam-thermal reactions are significant. When the density is much lower and the temperature is much higher than these cases, the beam-beam reactions become significant (Figs. 6(e) and 6(f)). Of interest here, the $\theta_D - \theta_T$ dependence of the beam-beam fusion shows maxima at $|\theta_D - \theta_T| \approx 0.7$ as indicated by arrows in Fig. 6(f). This can be interpreted by the velocity difference between the slowing down beam components. At certain injection angle difference, the relative velocity difference between D- and T-particles, which forms a cone-like distribution in three dimensional velocity space, tends to be the optimum (see circles in Figs. 5(b) and 5(d)).

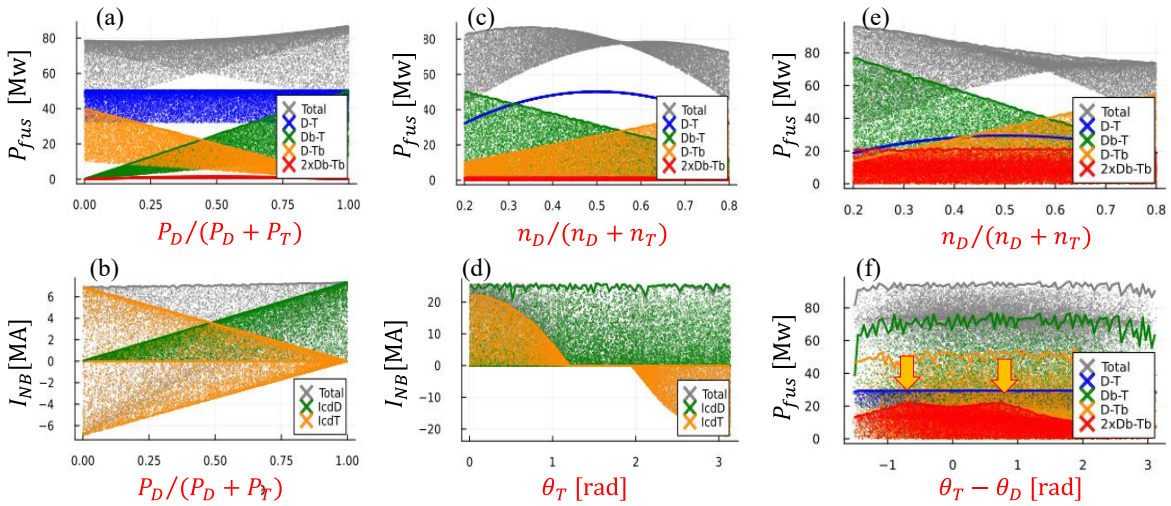

FIG. 6. Fusion power P_{fus} as a function of $P_D/(P_D+P_T)$ (a), as a function of $n_D/(n_D+n_T)$ (c) (e) and as a function of $\theta_D-\theta_T$ (f). NBI driven plasma current I_{NB} as a function of $P_D/(P_D+P_T)$ (b) and as a function of T-NBI injection angle θ_T (d). Figs. (a)-(d) show the case with parameters: $n_e=1.2\times10^{20}\ 1/m^3$, $T_e=T_D=T_T=12.5\ keV$, $E_{beam}=450\ keV$. while Figs. (e), (f) show the case with parameters: $n_e=0.5\times10^{20}\ 1/m^3$, $T_e=T_D=T_T=30\ keV$, $E_{beam}=100-800\ keV$. Different colors represent the contributions of different components, while gray points represent the total.

5. SUMMARY

FAST is a project being proposed in Japan as a facility for R&D, testing, and demonstration of systems integration for a DT fusion energy reactor. A quasi-zero-dimensional parameter survey was performed to optimize the design point for FAST that satisfies its requirements (P_{fus}= 50–100 MW, neutron wall loading of 0.3–1 MW/m^2, discharge duration of 1000 s, and full-power operation lifetime of 1000 hrs) with a minimum device cost. A hybrid energy confinement time scaling was used, which results in the optimum aspect ratio of A ~ 2.2. The optimum A was weakly affected by the choice of the interpolation method between low A and conventional A scalings. The device cost was estimated from the unit volume cost of each component, and the NBI cost is added. Since the NBI cost is a significant fraction of the total cost, the optimum parameter set is weakly affected by the relative cost of NBI. The survey results showed that a compact (major radius ~2.0 m) tokamak with HTS magnets and NBI power of about 50 MW (with the energy of 500 keV) offers a possible design window when we require $n_{Wmax}=0.7$ MW/m^2 and $P_{fus}=70$ MW. These parameters are derived as a result of choosing HTS magnets with a thin shield of about 0.4 m. The device cost analysis shows that the combination of the target n_{Wmax} and P_{fus} should be constrained around the cost-valley curve (Fig 4(a)) for cost-effectiveness.

NBI is the main heating and current drive tool, and beam-thermal DT reaction is significant. Therefore, the design should be optimized considering the reaction. So far D-NBI to T-rich target seem to be preferable, but more detailed and comprehensive analysis is necessary.

The design window of FAST seems to be located between a beam-driven neutron irradiation reactor and a demo reactor. A high energy gain, a high tritium breeding ratio and a long operational period are not mandatory, which lead to a new parameter set region, and probably result in a short construction period and a small cost.

REFERENCES

[1] FAST projects (2024), https://www.fast-pj.com/en .
[2] Ejiri, A., et al., "Optimization of design point for a fusion energy systems integration test facility FAST", Plasma Phys. Contr. Fusion **67** (2025) 075002.
[3] Menard, J.E., "Compact steady-state tokamak performance dependence on magnet and core physics limits", Philos. Trans. R. Soc. A: Math. Phys. Eng. Sci. **377** (2019) 20170440.
[4] Okano, K., "Neoclassical formula for neutral beam current drive", *Nucl. Fusion* **30** (1990) 423.

[5] Hazeltine, R. D. and Neiss, J. D. 1992 Plasma Confinement (Addition-Wesley Publishing).
[6] Huba, J. D., 2004 NRL plasma formulary revised 2004.
[7] Fujita, T, Sakai, R. and Okamoto, A., “Optimization study of normal conductor tokamak for commercial neutron source”, Nucl. Fusion **57** (2017) 056019.
[8] Sheffield, J. and Milora, S. L., ”Generic Magnetic Fusion Reactor Revisited”, Fusion Sci. Technol. 70 (2016) 14.